

# GNC for a Rendezvous in Space with an Uncooperative Target

Josef Sommer<sup>(1)</sup>, Ingo Ahrns<sup>(2)</sup>

<sup>(1)</sup> Astrium GmbH, Airbusallee 1, 28199 Bremen, Germany, +49 421 539 4440,  
josef.sommer@astrium.eads.net

<sup>(2)</sup> Astrium GmbH, Airbusallee 1, 28199 Bremen, Germany, +49 421 539 4010,  
ingo.ahrns@astrium.eads.net

**Abstract:** This paper describes a conceptual GNC system layout and presents preliminary performance results for a rendezvous with a disused but known space vehicle, i.e. the knowledge of the S/C geometry is exploited by the navigation dedicated onboard image processing. First the typical mission segments and corresponding GNC requirements are summarized. Thereafter a preliminary GNC system layout for the chaser spacecraft in accordance to the mission needs is presented. For the GNC description focus is given to the image based navigation over the complete approach distance. In the proposed concept, a video camera has been selected as the primary navigation sensor for far range distance, a laser scanning system (3D-LIDAR) provides the required measurements for mid-range and the same sensor, while operating in the 3D modus, serves as the primary sensor in close range distances. In the 3D modus the 3D-LIDAR provides a point cloud, which is used for pose estimation. The preliminary performance of the image processing algorithms has been tested in both, a simulation environment and with real sensors in a test facility. Finally the laboratory environment for navigation design and analysis including the use of a test facility for sensor testing is briefly described.

**Keywords:** *Rendezvous, uncooperative target, GNC system layout, vision-based navigation, 3D-LIDAR*

## 1. Introduction

Since the first manually controlled rendezvous and docking between the Gemini capsule and the unmanned Agena vehicle in March 1966, the rendezvous in space more and more has become a standard maneuver. Already in 1967 the first automatic rendezvous and docking between two Kosmos space vehicle took place on the basis of radar tracking. Advancements of these systems have been applied over decades in the regular visits and servicing for the operation of different space stations. However, the existing and well proven systems suffer technical obsolescence, are heavy, expensive and require relatively high energy. Therefore almost all space agencies are working on new systems exploiting modern sensor systems and high performance computer systems. Many of the new developments have been tested in demonstration flights (ETS, XSS, DART, Orbital Express, PRISMA). Not all of them were successful thus underlining, that still the rendezvous in space is a complex and risky maneuver. In the new developments optical sensors (video, laser, PMD) are preferably applied for the close range navigation (order of 100m). For the far range distance (order of km) in low earth orbits, space based navigation system like NAVSTAR GPS, GLONASS or Galileo with its low cost high performance receivers are the preferred solution. With the first

successful rendezvous of Jules Verne (ATV 1) with the ISS on April 3rd 2008 also Europe has proven its capability for automatic rendezvous in space. Here optical sensors (scanning LIDAR, laser camera) and a simple kind of image processing (target pattern evaluation) have already been applied for the close range measurements [1]. Common to all addressed systems is that the target behaves cooperative, i.e. it supports the coupling by dedicated docking/berthing systems and the navigation by means of a communication link (RGPS) and navigation aids like target pattern. Moreover the target is controlled thus being able to establish an attitude convenient for the approach and docking.

For satellites at the end of life or incapacitated space vehicle the cooperativeness for the rendezvous is not given. The spacecraft is passive, i.e. no active attitude control, no information about its position and target pattern or dedicated mechanism for coupling. Moreover the vehicle may tumble in an arbitrary manner with rates in the order of a degree per second. Hereafter an approach strategy and a system are presented which shall enable the rendezvous with an uncooperative and tumbling target in a low earth orbit. It is assumed however that the geometry of the target is known.

## **2. Reference Mission**

The reference mission selected for the system layout corresponds to a servicing or disposal of space vehicle in low earth orbit, i.e. it is a single dedicated mission. Similar to the well known rendezvous with a cooperative target (e.g. ATV with the ISS, see [1]) the mission may be decomposed in:

- Phasing (orbit synchronization between chaser and target)
- Approach based on relative navigation
  - Homing (target acquisition by the far range sensor (Rendezvous Entry Gate) and autonomous control of the relative distance by the chaser (formation flight))
  - Closing (approach up to an inspection flight around the target)
  - Final approach (close range approach up to the mating point using pose estimation of the target)
- Capture & Servicing
  - Grappling, mating, stabilization and alignment of the coupled system
  - maintenance / refueling or
- De-orbiting (initiation of a controlled re-entry)

The kernel onboard functions for the execution of such a mission are the GNC and the capture system. In the investigated concept the latter is given by a manipulator system being in charge of grappling and stabilization. In the following focus is given to the major elements of the GNC system, namely rendezvous sensors, actuators and the algorithms.

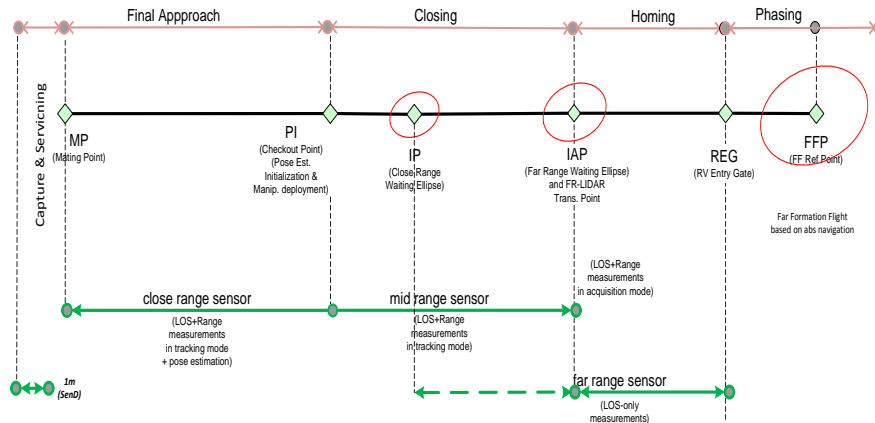


**Figure 1. Mission Phases**

Except for the phasing all mission phases mentioned above shall be performed automatically, though it may be possible to intervene from ground in critical situations (see figure 1).

For the phasing the knowledge of target orbit is needed. This is derived from ground based radar tracking data. All larger artificial earth orbiting objects are tracked by NORAD and catalogued such that the available TLE of the target can be used as a starting point. At the end of the phasing a dedicated radar tracking campaign, e.g. by the TIRA system in Wachtenberg near Bonn, Germany, may be applied to reach relative positioning accuracy compliant with the onboard relative measurement sensor. Depending on the sensor, the distance for relative measurement acquisition may vary between around 1km (or less) and several 10km.

Once the target has been successfully acquired by the far range onboard sensor, the homing guidance starts working for the acquisition of a formation flight in several hundred meter distance to the target. The formation flight needs to be automatically controlled in a safe manner with low fuel consumption. In this configuration the GNC system is checked out for the further approach and convenient conditions (illumination, ground contacts) may be waited for.

When the system is OK and the mission conditions are met, the approach (closing) to the inspection flight is initiated. Up to this phase the guidance exploits orbital mechanics to ensure safe trajectories and low fuel consumption for the approach.

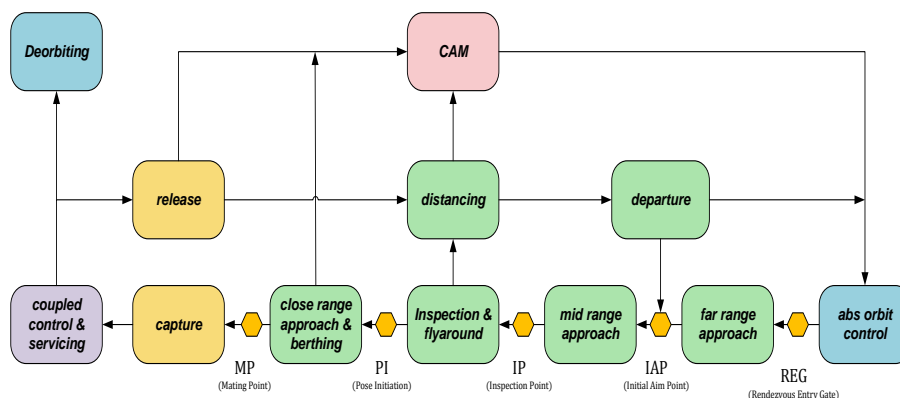


**Figure 2. GNC Functions**

For the close range approach the geometry and the attitude motion of the target generally needs to be accounted for in the relative measurements. The selected strategy strongly depends on the capture system and the size of the target. For smaller targets w.o. large appendices the close range approach can be performed w.o. the need of a dedicated synchronization between the target attitude motion and the chaser positioning. In this case a manipulator system can capture the target and damp out the relative motion up to rigidization. Then, after realignment of the composite, the target is moved by the manipulator arm such that a de-orbitation boost can be applied.

For larger targets like Envisat with large appendices (antenna, solar arrays) this is possible only when the tumbling rate is very small or allows an attitude independent approach. Generally in this case the chaser must synchronize its motion with the target attitude motion to avoid a collision with the appendices, i.e. the last meter approach is performed w.r.t. a target fixed reference system before the manipulator arm is grappling an appropriate structural element of the target. Thereafter the coupled system is stabilized and aligned to respect thermal constraints and ensure communication.

For de-orbitation and subsequent controlled re-entry in the earth atmosphere delta-V manoeuvre of more than 100m/s are needed. This requires a thrust vector through the centre of mass of the coupled system. Once the c.o.m. has been determined by a set of appropriate maneuvers, the target/chaser composite can be adjusted by the manipulator system such that the orbit control system of the target can conduct the necessary delta-V maneuver(s). The thrust level must be large enough to achieve a sufficiently large entry angle to meet the reentry constraints for a sufficiently small splash down area.

### 3. System Concept

Both, for servicing of malfunctioning satellites and disposal of disused or broken space vehicles a number of different concepts have been analyzed in the past.

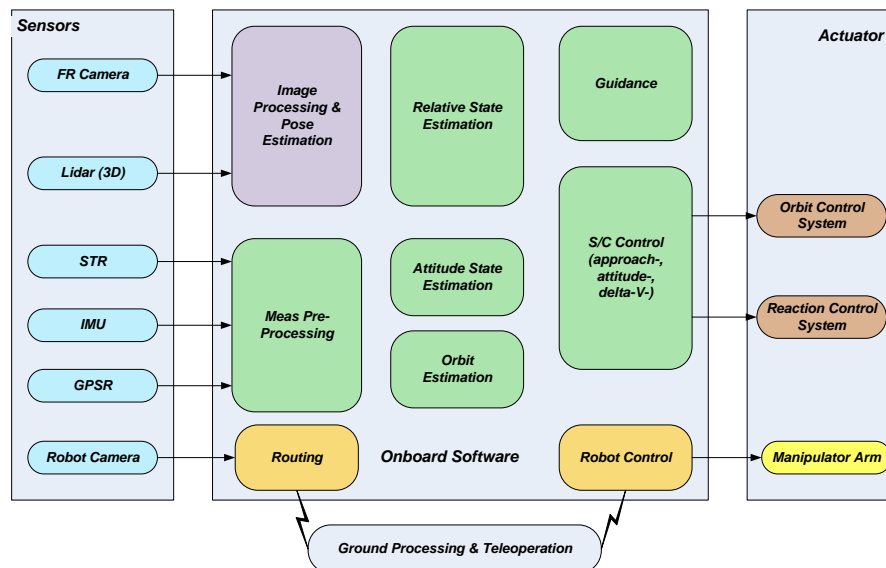


Figure 3. GNC System Concept

New and critical assemblies in these concepts are given by the navigation- and the capture system, but also new actuation concepts like the electrodynamic actuator or drag increasing mechanism have been investigated. For a controlled reentry however relatively high acceleration levels are required so that these concepts do not provide an alternative to chemical thrusters.

As described above, the reference scenario is a single dedicated servicing/disposal mission of a small compact space vehicle. The capture system is assumed to be a lightweight manipulator arm, which is able to grapple a tumbling satellite and smoothly damp the relative motion between target and chaser. The description hereafter is focused on the GNC system not including the manipulator control.

Besides the specific RVD sensors and a dedicated capture mechanism, the GNC system requires standard attitude sensors (rate measurement unit, star sensor, GPS receiver) and a reaction control system which is able to provide linear torque free acceleration in each body axis for position control. Figure 3 shows the functional block diagram of the envisaged system, including a major partitioning of the GNC algorithm. The robotic manipulator system with a potential control loop via ground has been included for the sake of completeness.

### **3.1. The Actuator System**

The choice for the reaction control system very much depends on the mission duration. In case of a short dedicated mission, fuel consumption for attitude control is of minor importance and does not justify the use of reaction wheels and/or torquer. Like for the ATV it is then more efficient to apply a thruster based reaction control system which must be able to generate torque free forces along and force free torques around each body axis. This is possible with a set of pulse commandable thrusters controlled by a dedicated thruster management function to find the fuel optimal combination for a given force/torque command.

For the large orbit transfer maneuver and re-entry thrusters with a sufficiently large specific impulse and a sufficiently high thrust level are needed. This is given by classical chemical thruster (mono- or bi propellant) available for thrust level between 1N and 500N with a specific impulse between 220 and 320s. The servicer total mass is assessed with about 1t, i.e. control accelerations in each axis of about 2mm/s<sup>2</sup> are available.

For long lasting or multi servicing missions, the fuel needed for attitude control is not negligible and the use of reaction wheels and torquer pay off in the mass budget and cost. For a chaser mass of around 1t small wheels with about 10Nms and torquer of about 70 Am<sup>2</sup> dipole moment are considered sufficient.

### **3.2. The Sensor System**

In addition to the classical AOCS sensors (IMU, STR, GPSR) the sensor system comprises specific sensors for position measurements relative to the target. Candidate sensors for the far range are cameras (optical, infrared) or radar, which are able to provide line of sight or range or both measurements. Active sensors like radar or laser are limited (order of km) in their measurement range by the affordable power, optical or

infrared sensors are limited by the chaser visibility. In [10] it was shown that even small targets can be detected in distances larger than 20km, which makes the camera sensor an inexpensive far range sensor. The navigation performance however generally is poor since only line of sight measurements are available. Moreover for a big part of the orbit the target is not visible due to eclipse or sun in the sensor field of view. During these periods pure relative orbit propagation is needed.

For the mid-range distance the navigation performance based on LOS measurements is insufficient and range and potentially range rate measurements are added. This can be achieved with RADAR, a laser scanner or a stereo camera system. A stereo camera system would need a rather large baseline for position measurements, a standard radar systems will not work in close range distances with sufficient performance. A laser scanner provides high measurement performance in mid and close range distances, and when operating in 3D mode, it allows the derivation of the chaser pose for the final approach (see paragraph 3.3.2). This is important since for a tumbling chaser the range measurement depends on the attitude of the chaser and needs to be accounted in order to avoid an undulation in the position control.

### **3.3. GNC Software**

The GNC software is in charge of the processing of the sensor measurements, the computation of the flight trajectory, the navigation, the attitude and position control as well as the flight control and safety monitoring.

#### **3.3.1 Guidance**

The autonomous flight control starts at the end of phasing, when the far range camera has acquired the target and the navigation filter indicates convergence. For the present concept it is assumed, that at the end of the phasing ground-based radar tracking campaign and relative orbit determination has been performed, which gives pretty good initial knowledge for the onboard state estimation and allows the initiation of a drift towards the target. If the tracking campaign shall be omitted the onboard system must rely on NORAD data for the target, the accuracy of which very much depends on the age of the TLE. It certainly requires a target acquisition at distances larger than 10km and needs an according visibility and navigation performance analysis, when a camera will be used in this phase (see also [10]).

Both, the approach and the formation flight apply e-i-separated trajectories described in relative orbital elements (see [8]). The figure below shows a transition from a far formation flight (here about 6km) based on absolute navigation to a mid-range formation flight based on 3D-LIDAR measurements at around 1km

Once the target is seen by the camera the size of the walking-ellipse is stepwise decremented in accordance to the improving navigation accuracy when approaching the target. Since atmospheric drag and gravitational anomalies are disturbing the approach trajectory regular correction maneuver are necessary to reach the IAP with sufficient accuracy. At the end of this transition a formation flight is established at a distance where 3D-LIDAR measurements are available and the 3D-LIDAR sensor takes over the role of the primary GNC sensor for rendezvous.

For closing, including the inspection flight the e-i-separation guidance strategy is kept. In fact, the inspection is a formation flight at about 50m distance with the target in the center of the ellipse

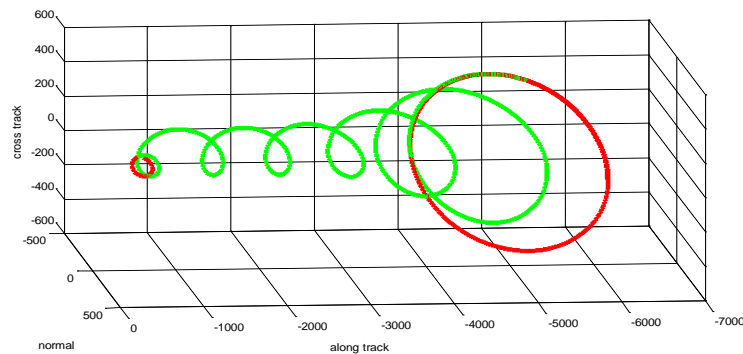


**Figure 4. Formation Flight and Spiral Approach**

After the inspection a hold point on the V-Bar about 20m behind the target is acquired. In this point the 3D-LIDAR mode is switched to 3D and the pose estimation is initiated. Based on the inspection results, the approach direction towards the target is defined. Since the V-Bar approach is advantageous in terms of complexity, flexibility (easy introduction of further hold point) and fuel consumption this is selected whenever possible. Alternatively a fly around may be required to reach a different approach axis towards the target.

### 3.3.2 Navigation

The navigation function provides the position and attitude state vectors for guidance and control. The attitude estimation is based on a classical Kalman filter fed by gyro and star tracker measurements. For the derivation of the LVLH attitude the chaser absolute position information from the GPS receiver is used. For the estimation of the relative position and velocity three major modes are distinguished: i) based on line-of-sight (LoS) measurements only (camera), ii) based on LoS and range measurements (3D-LIDAR), iii) based on a point cloud provided by the 3D-LIDAR in 3D mode.

In [3] a comparison of appropriate filter techniques for the relative navigation was conducted showing that complex filter techniques (particle filter, UKF) are not much better than standard Kalman filtering. Since the guidance for the formation flight and the spiral approach is formulated applying relative orbital elements and since this model allows easy incorporation of  $J_2$  and air drag, this model is applied for the far range navigation. For the mid- and close-range navigation with the 3D-LIDAR the HCW (Hill Clohessy Wiltshire) formulation delivers directly a state estimation w.r.t. the LVLH.

For the state estimation with LoS measurements only, it is not sufficient to have good illumination conditions. Strictly speaking observability is reached only by maneuver, which change the visibility geometry of chaser and target. Thanks to the spiral approach concept this is given. In fact it appears that several small maneuvers are better than few large ones, though the instantaneous variation is rather small. Also radial and out of plane maneuver are more effective than along track maneuver, which is also supported by the guidance strategy. The simulated navigation performance along a typical spiral approach was analyzed applying a camera with a  $4^\circ$  FoV and a resolution of  $1024 \times 1024$

pixels. Though large parts of the orbit are without measurements, a  $1\sigma$  performance of about 50m along track and about 10m cross track and out of plane is possible. Similar results have been achieved by DLR-RB with the ARGON experiments on PRISMA (see [10]).

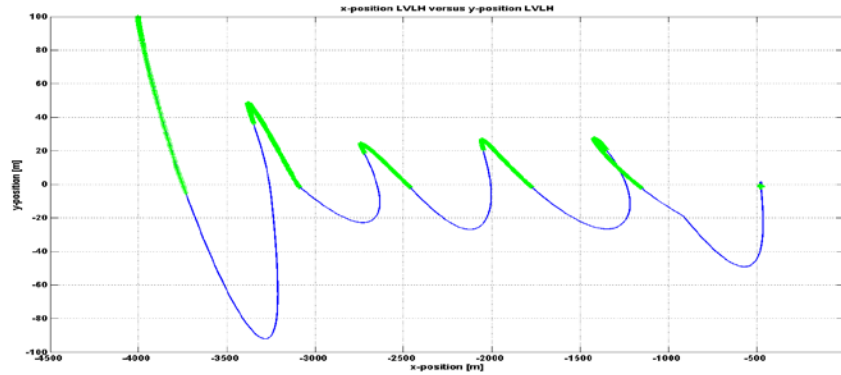


**Figure 5. Measurement periods (green) during the spiral approach**

With the availability of range measurements the relative state vector is fully observable and the estimation performance drastically increases. Figure 6 shows the estimation error with the following assumptions about 3D-LIDAR performance:

- Total scanning FoV:  $40^\circ \times 40^\circ$
- Scan / Tracking Window Size:  $1^\circ \times 1^\circ \dots 40^\circ \times 40^\circ$
- Range accuracy (Bias):  $1.4\text{m} @ 1400\text{m} \dots 5\text{cm} @ 1\text{m}^*$
- Range accuracy (Noise, 3 sigma) :  $0.6\text{m} @ 1400\text{m} \dots 2\text{cm} @ 1\text{m}^*$
- LoS accuracy (Bias):  $\pm 0.05^\circ$  (fixed target surface)
- LoS accuracy (Noise, 3 sigma):  $\pm 0.02^\circ$  (fixed target surface)

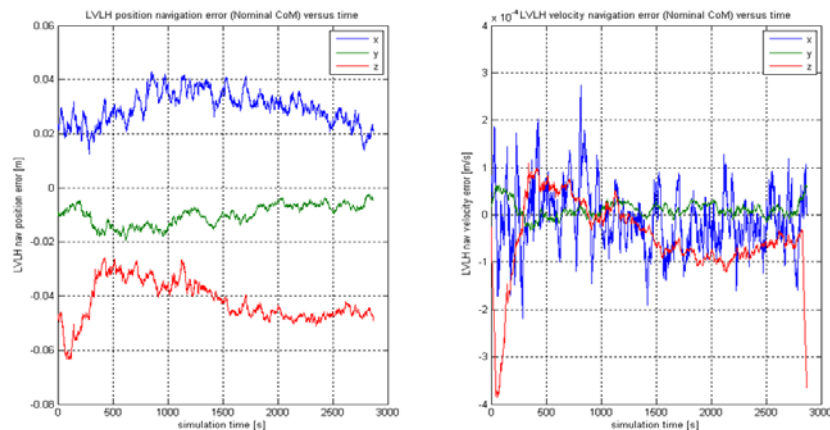


**Figure 6. Simulated 3D-LIDAR based navigation error during mid-range approach**

Here the position error is in the order of cm and thus allows a safe approach to the PI. For the close range the averaging of the range measurements within the LIDAR may result in significant errors, depending on the target tumbling motion and the target geometry. Therefore the individual measurements of the 3D-LIDAR scan (point cloud) are taken by the vision-based navigation, from which the target pose is estimated w.r.t.

the sensor frame. This is easily transformed into the LVLH reference frame, thus providing high performance relative position (and velocity) information independent of the actual target attitude.

For the evaluation of the 3D LIDAR data (point cloud) a strategy consisting of two subsequent processing steps is applied. First, an initialization of the pose is performed by applying a correlation between a dataset of reference views extracted with the current view of the target extracted from the LIDAR scan (typically small images of 30x30 points are used for the correlation). Based on this template matching technique, first rough pose estimations in the order of several centimeters and  $\pm 5^\circ$  attitude error can be obtained. In order to refine this first rough pose estimation, further iterative steps applying an iterative closest point algorithm (ICP) [12] are used.

The following diagram in figure 7 shows the results of these two stages. Figure 7 (a) represents the angles of 1296 different viewing directions showing the full test sets. Figure 7 (b) shows the error distribution for the application of the correlation based initial pose estimation for the ENVISAT model. The peak around  $0^\circ$  for all three angles indicates the large number of cases where the correct initial pose has been found by the first pose estimation stage.

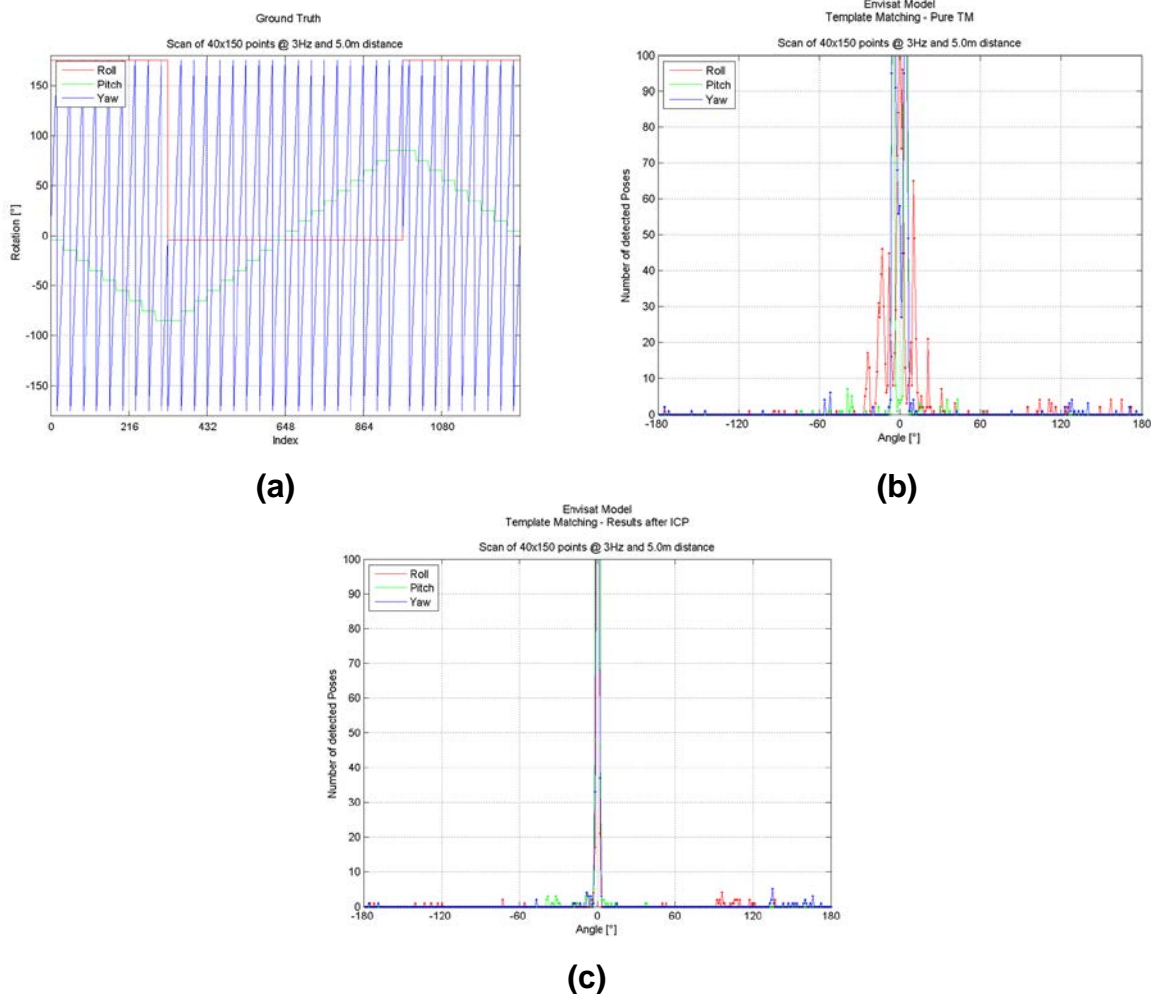


**Figure 7. Performance of pose initialization stage based on 3D-LIDAR measurements.**

Figure 7 (c) finally depicts the final accuracy that has been achieved when using the coarse pose estimation of the first stage for the initialization of the second ICP stage. The first stage only has to estimate the pose of the target object such that the solution falls into the radius of convergence of the second stage.

The next diagrams show a test case for the approach of the Envisat model for a typical forced-motion trajectory starting at a distance of 50m going down to approximately 3m.

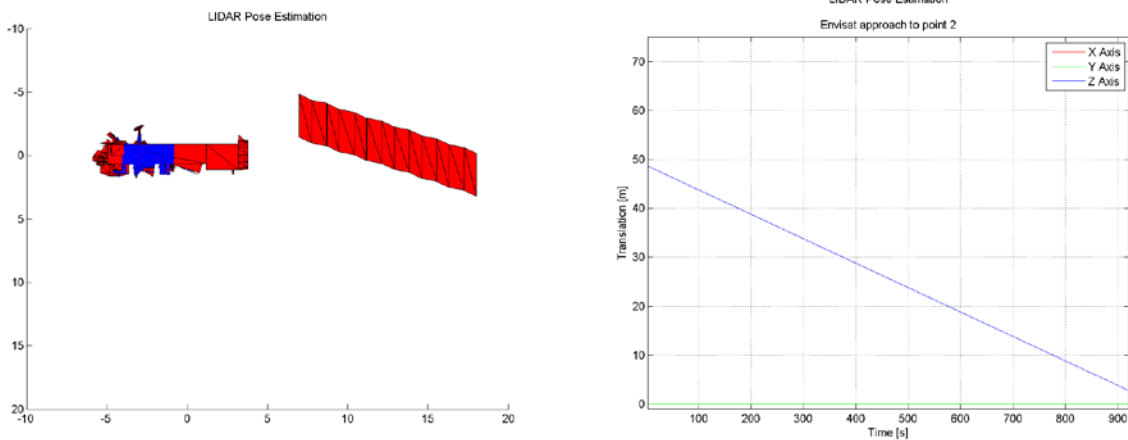


**Figure 8. Approaching the ENVISAT model starting at 50m distance.**

The next two diagrams depict the achieved pose estimation performance (without applying any further filtering).

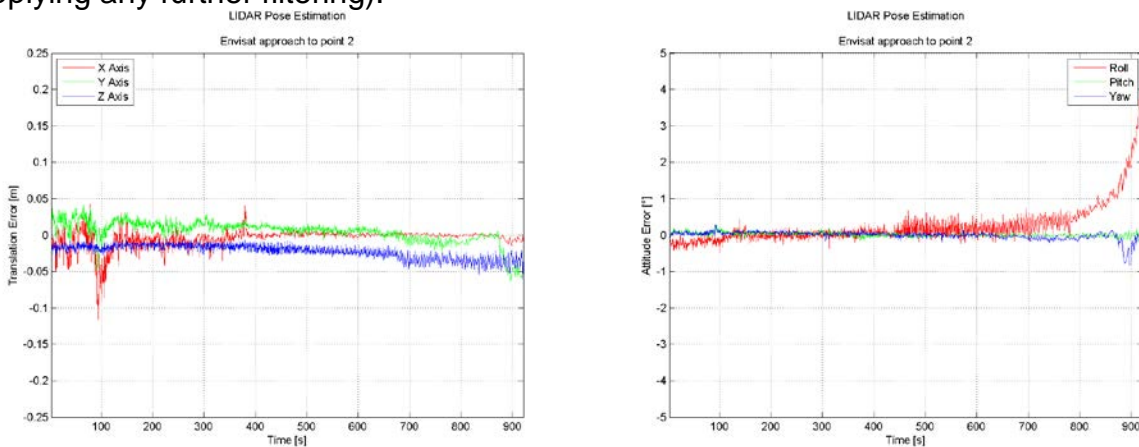


**Figure 9. Pose estimation performance during Envisat approach.**

The pose estimation accuracy is in the order of few centimeters for the position and less than one degree for significant distances to the model. As soon as the geometry in the limited field of view of the 3D-LIDAR does not show sufficient spatial structure, the performance degrades, indicating that a minimum distance between chaser and target has to be taken into account. This minimum distance depends on the size and the geometry of the target object. For the specific test point and the size of Envisat, this distance was approximately 5m (distance between sensor system and Envisat center of mass corresponding to a sensor to surface distance of approximately 3m).

The single pose estimations can then be used to feed a Kalman filter that takes into account the tumbling motion character of the target object. The system equations of the Kalman filter just model the linear approach velocity of the chaser to the target and the tumbling motion (in case of the absence of external forces as it might be commanded during an observation phase for motion estimation). The tumbling motion is simply modeled by the well-known Euler equations of tumbling rigid body motion. The pose estimations are treated as measurements although an optimization stage is necessary to obtain these pseudo-measurements. Based on these input data it is possible not only to estimate the pose, the velocities and angular rates but also the ratio between the moments of inertia of the target object which determine the evolution of the angular rates according to the Euler equations. Based on the estimated motion parameters it is possible to feed a path planner for a manipulator mounted on the chaser. Such a path planning applies the estimated motion parameters to predict the expected position and attitude of the chaser at a specific future point in time for which a grasping manoeuver is foreseen. The following two diagrams in figure 10 show the results of the Kalman filter applied to single pose estimations. Especially the convergence to the correct ratios of the moments of inertia can be observed. The convergence is achieved even for the unlikely case that no a priori knowledge about the moments of inertia exists. In this case all three values have been initialized with 1.

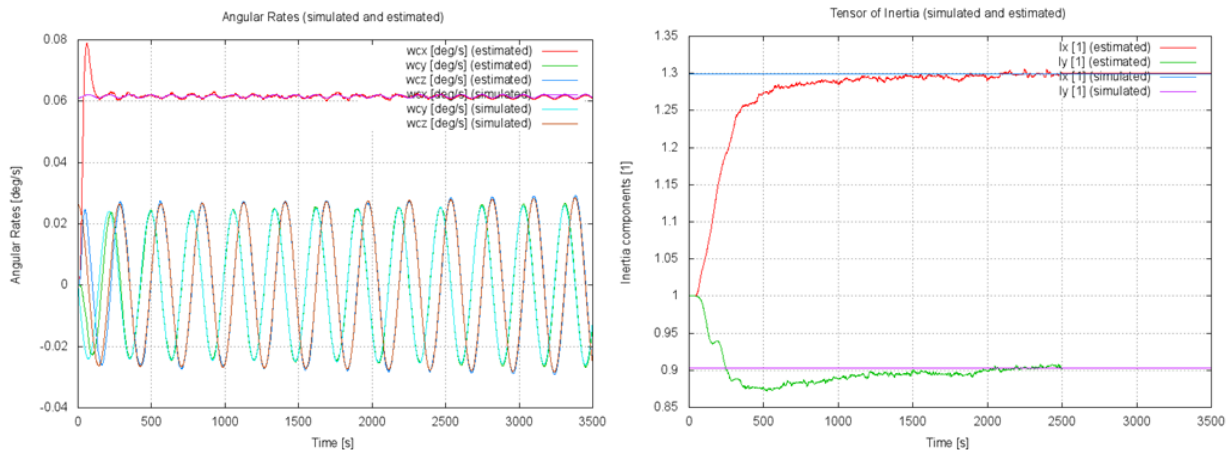


**Figure 10. Motion estimation based on single pose estimations.**

### 3.3.3 Control

Like for the attitude estimation, the control to a large extent relies on proven methods from the ATV design. The attitude control is performed with a configurable PID controller. The same principle holds for the position control in close range. The resulting force/torque command vector is processed by a thruster management function to find the best (fuel minimizing) combination of thruster firing for its realization. For far and mid-range regular correction maneuver are computed by comparing the actual relative orbital elements with the ones required by the guidance.

### 3.3.4 Flight Control Monitoring

The Flight Control Monitoring (FCM) shall ensure correct functioning of sensors, actuator and the GNC algorithm. In addition to the standard FDIR task this includes coherence checks by analytical redundancy, performance monitoring of the navigation filter and trajectory monitoring w.r.t. safety constraints. The latter may trigger a collision avoidance maneuver (CAM) when the collision risk appears too high.

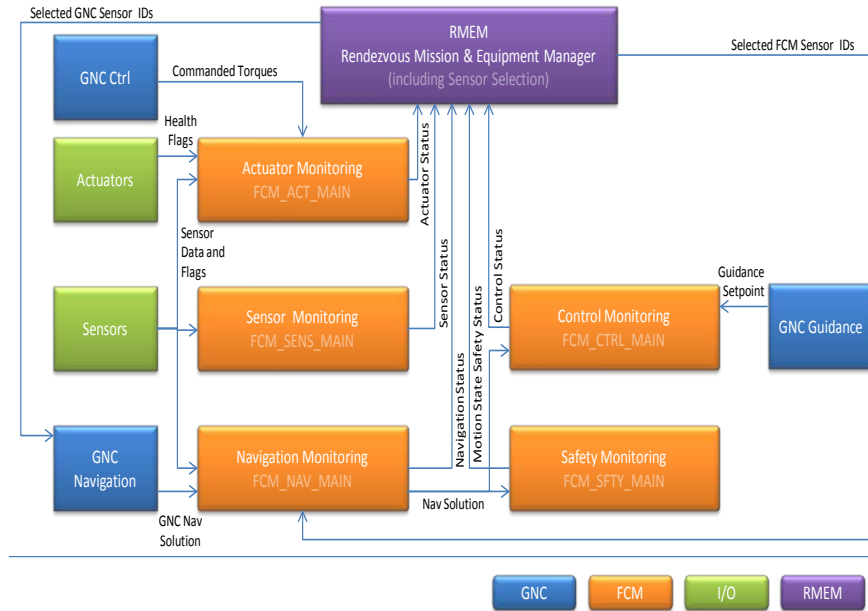


**Figure 11. Flight Control Monitoring Block Diagram.**

The sensor monitoring evaluates the health information provided the sensors (BITE) and checks the received measurements w.r.t. plausibility. The navigation monitoring evaluates the filter internal performance estimation (innovation monitoring) and compares, where possible state vector information from different sensors (e.g. 3D-LIDAR vs. camera). The control monitoring evaluates the control error and the controller output (saturation, activity). The actuator monitoring evaluates the consistency between thruster commands and measured reaction by inertial sensors

The safety monitoring checks the estimated state vector against a collision risk by state and error propagation. In case of an impending collision, a CAM is triggered

All monitoring functions provide the detection results to a recovery logic within the mission and vehicle management. The recovery action may simply activate the redundant system, interrupt the approach or abort the approach with a CAM.

### 3.3.5 Collision Avoidance

Two strategies are implemented for collision avoidance, passive safety by flying e-separated trajectories in far- and mid-range, and active collision avoidance maneuver in close range. For the passive safety an appropriate radial and out of plane distance to the target trajectory is imposed such, that in case of loss of control the error ellipsoid is not touching the target envelope for at least five orbits. In the close range this would trigger frequent alarms. Therefore the estimated state vector is compared to a corridor around the expected nominal values. If a limit is exceeded a CAM is triggered.

Different to the CAM of ATV, the proposed one consists of two maneuvers as applied in [9]. The first maneuver is selected such that the chaser is reaching a predefined minimal distance within a predefined time interval, and the second maneuver stops the imposed drift and imposes an appropriate e-i-separation so that a trajectory similar to the one shown figure 12 is established. The result is a trajectory with a large radial and out of plane distance to the target and low drift. This keeps good initial conditions for failure analysis and re-initiation from ground.

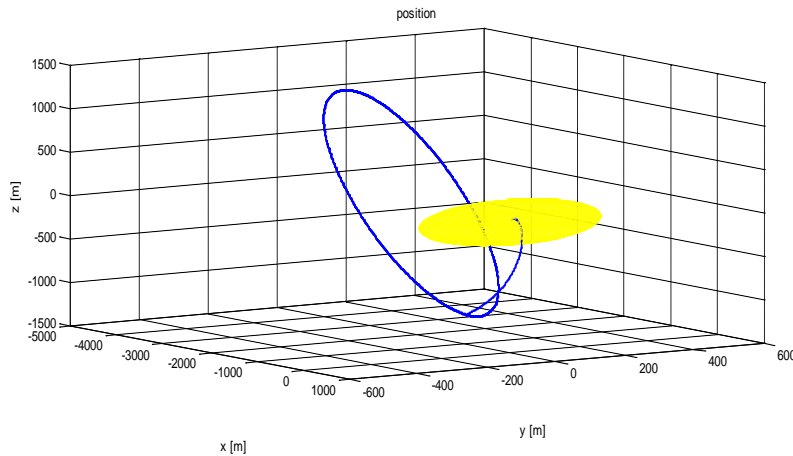


**Figure 12. Typical CAM Trajectory.**

#### 4. Verification

A key element in the verification is the simulation. Along the development there are a number of different simulators needed, depending on the use cases, being a function of the development-, test- and operational phases.

It is obvious, that a consistent simulator concept with strong reuse of components from one phase to the next (e.g. from the development phase to SW verification, system AIT and even the operational phase) is the most cost effective and recommended way. Components from the early development phase shall be portable to the successive validation phase with small effort. Enhancements for specific test environment shall be applied such, that the kernel remains unaffected. The envisaged approach essentially follows the definitions and use cases of the ESA standard [11]. Functional Engineering Simulator (FES): The FES support functional and algorithm performance validation of the GNC. It reflects the architecture and functional interfaces of the system and provides representative models for the dynamics, perturbations, sensors and actuators. System requirements and algorithm performance are verified by simulation.

Rapid Prototyper (RP): The RP-System is used for the validation of the system concept in a real time environment, which represent fully or partially the real system behavior (e.g. test facility). It is not necessary to apply the target hardware but high performance commercial real time systems like dSPACE can be used (see figure 14). The focus is given to a verification of the functional requirements under real time constraints, without suffering the limitation of the target platform

Functional Validation Testbench (FVT) is applied for performance tests and validation of the GNC application software. This may include tests of H/W breadboards. In addition to the representativity of system architecture and functional interfaces (FES) the simulator

contains protocol and I/F specific adaptations (cradle) to incorporate the subsystem under test

Software Validation Facility (SVF) shall support the validation of the onboard software. It allows the conduction of integration-, I/F-, performance- and functional tests of the OBC software in open- or closed loop. The test facility either is equipped with an engineering model of the onboard or emulates the target computer. For the closed loop tests an environment simulation (models for dynamics, perturbations, sensors and actuators) is also necessary. When configured as a real time system it allows classical HIL tests.

Ground System Test Simulator (GSTS): The GSTS allows the ground segment verification against the system requirements. It supports both, component tests and the incremental integration of the components to a complete ground system up to an end to end system test. In addition to this specific tests may be conducted during the running mission, e.g. communication tests for TM/TC channels. For the RVD GNC a dedicated console is foreseen to test the interaction between ground and space segment during the proximity operations.

Figure 15 shows the simulator evolution and application along the system development and verification.

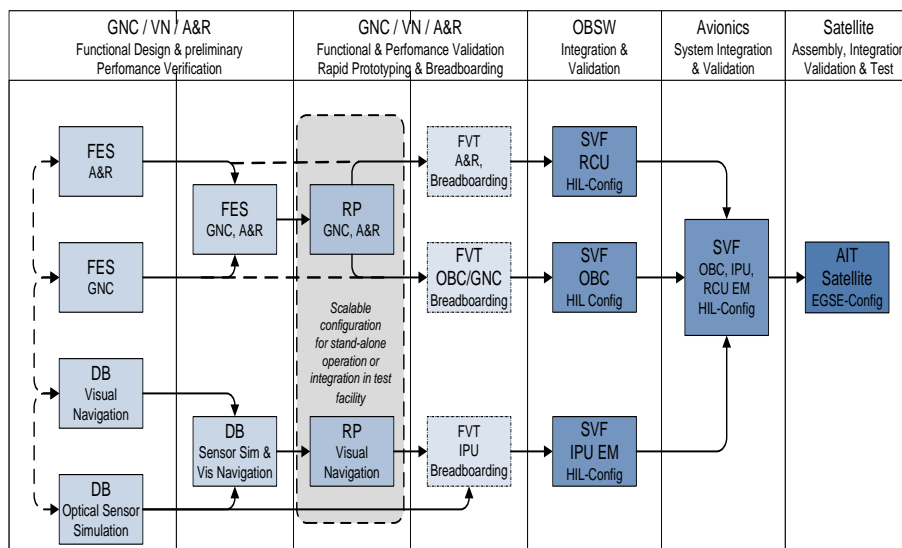


**Figure 15. Simulator Family.**

To become independent from imaging sensors and according sensor stimuli, a corresponding simulator shall generate representative camera and 3D-LIDAR raw data on the basis of simulated flight trajectories and target models (geometry and material). The quality of the simulated images shall be good enough to test the image processing algorithm w.r.t. sensor and target material specific characteristics

## 5. Conclusions

This paper proposed a complete conceptual GNC architecture for the rendezvous between a chaser and a non-cooperative target satellite and showed the main principles of the GNC subcomponents. First simulation results for all components have been presented, and, furthermore a strategy for the verification of such a complex system has

been presented. Special emphasis has been laid upon the navigation function based on camera and 3D-LIDAR sensor inputs. Vision based techniques have been proposed to be used for uncooperative targets and first results based on simulated sensor data of ENVISAT have been given.

## 6. Acknowledgements

The results presented in this paper essentially have been achieved in the scope of an Astrium internal project called INVERITAS. The work was performed between 2010 and 2012 and was co-funded by the German space agency „Raumfahrt-Agentur des Deutschen Zentrums für Luft- und Raumfahrt e.V.“ on behalf of the ministry of economy and technology, based on the funding initiative 50RA0908.

## 7. References

- [1] W. Ley, K. Wittman, W. Hallmann, Handbook of Space Technology, John Wiley and Sons, Ltd. Publications
- [2] W. Fehse, Automated Rendezvous and Docking of Spacecraft; Cambridge Aerospace Series 2003
- [3] A. Posch; Comparison of Filter Techniques for Relative State Estimation of In-Orbit Servicing Missions
- [4] D. Reintsema et al.; DEOS - The German Robotics Approach to Secure and De-Orbit Malfunctioned Satellites from Low Earth Orbit; iSAIRAS Konferenz 2010
- [5] J. Pearson; Active Debris Removal: EDDE, The Electrodynamic Debris Eliminator
- [6] L. Strippoli; Advanced GNC solutions for rendezvous in earth and planetary exploration scenarios; IAC-08-A3.I.15
- [7] S. Kerambrun; Autonomous Rendezvous System: The HARVD Solution; GNC 2008 (7th international ESA Conference on GNC)
- [8] S. D'Amico; Proximity Operations of Formation-Flying Spacecraft Using an Eccentricity/Inclination Vector Separation; Journal of Guidance, Control and Dynamics, Vol. 26, No. 3, May-June 2006
- [9] R. Larson; Orbit Constellation Safety on the Prisma in-orbit formation flying testbed; Proc. 3rd Int. Symp. on Formation Flying, Missions and Technologies, Noordwijk, The Netherlands, 23-25 April 2008 (ESA SP-654, June 2008)
- [10] Advanced Rendezvous using GPS and Optical Navigation (ARGON), Experiment Executive Summary, Dr. S. D'Amico
- [11] G. Gaias, S. D'Amico, J.S. Ardaens; Angles-only Navigation to a Non-Cooperative Satellite using Relative Orbital Elements, AIAA ASC 12GGA
- [12] Besl, Paul J.; N.D. McKay (1992). "A Method for Registration of 3-D Shapes". *IEEE Trans. on Pattern Analysis and Machine Intelligence* (Los Alamitos, CA, USA: IEEE Computer Society) **14** (2): 239–256.